# Effect of the Type of Mineral Aggregate on the High-Temperature Creep of HTR-Concrete

**U. Diederichs**
*Institut für Baustoffe, (Massivbau und Brandschutz) Braunschweig, FRG*
**G. Becker**
*Hochtemperatur-Reaktorbau GmbH, Mannheim, FRG*

## INTRODUCTION

Within the scope of the research and development work for the prestressed concrete vessel of the HTR 500 High-Temperature Reactor mix design, manufacture as well as mechanical and thermal behaviour of the concrete have been comprehensively studied (Becker 1984). Of the concrete types analysed, a basalt concrete showed extremely favourable high-temperature characteristics while a concrete with Rhine gravel was characterised by a good workability. These two types of concrete were subjected to numerous tests, whereby the testing procedures were strongly related to the anticipated combined stress, temperature and moisture conditions in the real structure.

The principal stress-temperature regimes during construction, prestressing and service of the vessel are schematically shown in Fig. 1. Phase I refers to the load-deformation history during prestressing of the vessel. At time $t_1$ instantaneous elastic deformation occurs, followed by creep at ambient temperature. Phase II represents the first heating of the vessel up to long-term service temperature. In this phase ($t_2$ ... $t_3$) the socalled transitional creep governs the stress-strain response of the concrete. Up to time >$t_3$ the service temperature is reached and thermally steady state creep of concrete starts.

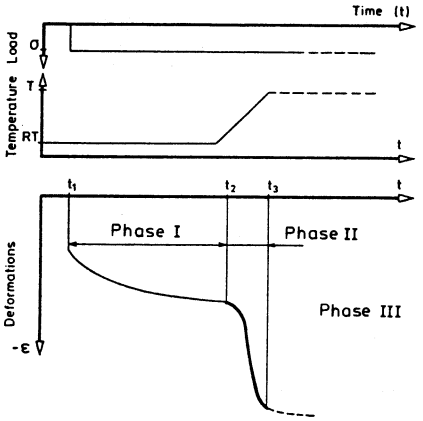


Fig. 1. Schematic load-temperature history and related concrete deformation of a reactor pressure vessel

Extensive experimental programs were conducted to study especially deformation behaviour and creep strength in the phase II (non-steady state thermal conditions), and at the beginning of phase III (constant elevated temperatures). From

these tests a lot of data concerning transient creep have been obtained (Diederichs (1986) and Diederichs & Ehm (1986)). This article presents a thorough evaluation of these results and verifies the effect of the different types of coarse aggregates on the specific creep terms.

## EXPERIMENTAL

The tests were performed with two HTR-concretes, Rhine gravel concrete and basalt concrete. Both concretes have nearly the same cement and fly ash content. The water/cement-ratio of the basalt concrete is a little bit higher than that of the Rhine gravel concrete. The "Rhine gravel concrete" contains continuously graded round, natural siliceous gravel from the Rhine area and natural sand; the basalt concrete is also made with siliceous sand and gravel, but half of the coarse aggregates is crushed basalt and the grading is discontinuous. Further details concerning the mix proportions are given by Diederichs (1986), Diederichs and Ehm (1986) and Weber et al. (1985).

The tests at elevated temperatures were performed with cylindrical specimens (diameter 80 mm, length 240 mm). The specimens were cast in metal moulds, demoulded after one day and stored under water for at least 90 days until testing. For testing the specimens were installed in a special testing facility comprising a pneumatic loading system (see Fig. 1) and equipped with thermocouples and dilatometer system. Then the specimens were loaded three times with 15 N/mm² to determine the modulus of elasticity at 20 °C.

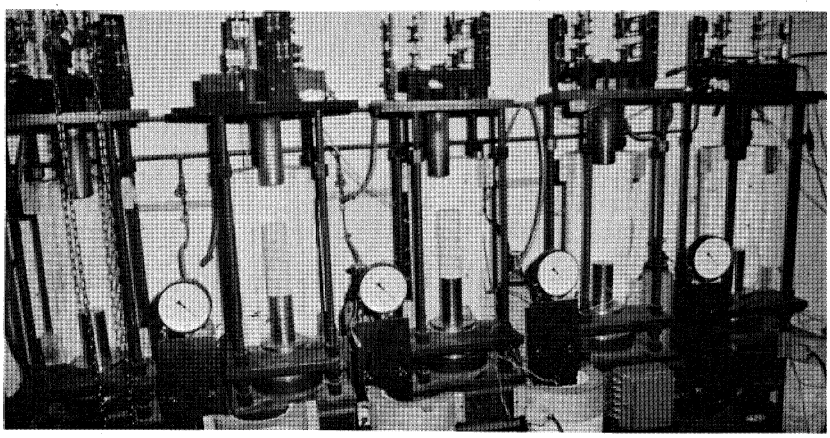

Fig. 2. Test facility for determining the deformation behaviour and creep strength of HTR-concrete

The specimens were then loaded with various load levels ($\alpha$ = actual stress $\sigma_o$/ultimate stress $\sigma_{ult}$) and heated unsealed immediately after loading with a constant heating rate up to the desired test temperatures (70 °C, 90 °C, 120 °C and 200 °C).

After reaching the test temperature, the load was maintained constant for further 30 days to get information concerning long-term steady state creep deformation and creep strength. Prior to cooling the specimens were again unloaded and loaded three times to measure the modulus of elasticity at high temperatures. After cooling the specimens down to room temperature $\sigma$-$\varepsilon$-tests were performed in a hydraulic testing machine as usual.

The applied load levels $\alpha$ were about 0.0, 0.02, 0.3, 0.5, 0.6 and 0.7, which cover the stress range 0.0 ... 45.9 N/mm². For each concrete and temperature-load level-combination three specimens were investigated. During the whole test-

ing procedure the surface temperature of the specimens and deformation were continuously recorded.

In Figs. 3 and 4 the complete set of measured total deformation data obtained during heating of basalt concrete and Rhine gravel concrete specimens is presented. The following comparative analysis concerns mainly these data, i.e. the concrete deformation during heating.

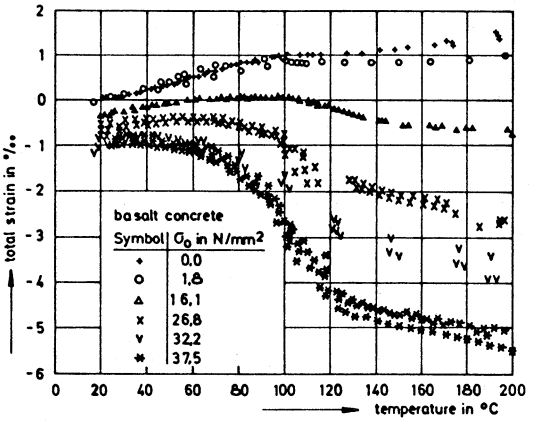


Fig. 3. Measured total deformations of basalt concrete during heating

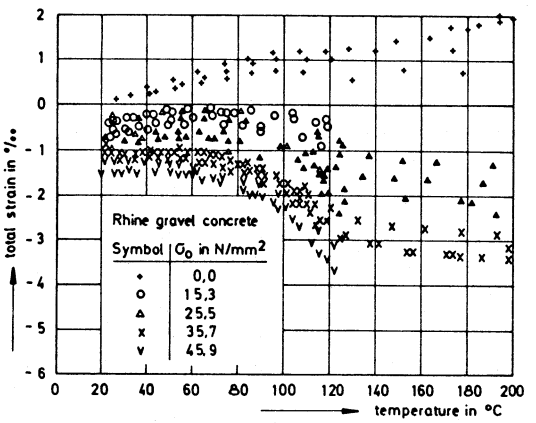


Fig. 4. Measured total deformations of Rhine gravel concrete during heating

## COMPARATIVE ANALYSES OF THE TEST RESULT

### Modelling of the Concrete Deformation at Transient Temperatures

In the literature the creep of concrete during the transition from one temperature to another is denoted transitional thermal creep or transient creep. It comprises the period of time in which the temperature field of a certain volume element of concrete is in the non-steady state. Therefore it is also often called non-steady state creep. - The respective creep data are to be determined from the experimental results of the above mentioned transient creep tests.

A number of complex material models have already been presented (see e.g. Anderberg & Thelandersson (1976), Khoury et al. (1985), Jumppanen et al. (1986), Schneider (1982) and Bazant & Panula (1979)), which describe the deformation behaviour more or less realistically. In nearly all models the total deformations ($\varepsilon_{tot}$) are divided into load independent thermal strains (= thermal expansion, $\varepsilon_{th}$) and load dependent strains ($\varepsilon_{\sigma}$):

$$\varepsilon_{tot} = \varepsilon_{th} + \varepsilon_{\sigma} \qquad (1)$$

whereby the components are considered dependent on multiple internal and external factors, e.g. concrete age at loading $\tau$, temperature T, moisture h, stress $\sigma$; their time derivatives $\dot{T}$, $\dot{h}$, $\dot{\sigma}$ and histories:

$$\varepsilon_{tot} = \varepsilon_{th}\,(\tau,\ T,\ \dot{T},\ h,\ \dot{h}) + \varepsilon(\sigma,\sigma(t),\ T,\ \dot{T},\ h,\ \dot{h}\ \ldots) \qquad (2)$$

The load dependent strain components are divided e.g. (see Anderberg et al. (1976)) into time independent, elastic and plastic deformations ($\varepsilon_{el}(\sigma,\ t)$) and $\varepsilon_{pl}(\sigma,\ T)$, transient deformations ($\varepsilon_{tr}(\sigma,T)$) and into time dependent creep strains $\varepsilon_{cr}(\sigma,T,t)$:

$$\varepsilon_{\sigma} = \varepsilon_{el}(\sigma,T) + \varepsilon_{pl}(\sigma,T) + \varepsilon_{tr}(\sigma,T) + \varepsilon_{cr}(\sigma,T,t) \qquad (3)$$

Schneider (1988) has presented a refined model:

$$\varepsilon_\sigma = \frac{\sigma}{E\,(E_0,\sigma,T)}\,(1 + \chi(\sigma,E,E_0) + \Phi(\sigma,T,h)) \qquad (4)$$

This model takes into consideration plastic deformation $\chi(\sigma,E,E_0)$, which can be usual observed in σ-ε-diagrams at high stresses. Furthermore, in this model the modulus of elasticity and the Φ-function are considered load and moisture dependent.

In Schneider's model (Schneider (1988)) as well as in the model of Bažant and Panula (1979) the modulus of elasticity plays a dominant role, because all other strain components are related to it. On the other hand, there is a complex interrelationship between the modulus of elasticity and the hygrothermal conditions, the testing methods and the evaluation method (see Jumppanen et al. (1986) and Diederichs et al. (1987)). Additionally, concrete behaves - particularly at higher temperatures - strongly non-linearly.

To illustrate the mentioned effects, the modulus of elasticity of a high strength concrete determined by different test methods is shown in Fig. 5 (see Diederichs et al. (1989)). The modulus of elasticity has been measured in three different ways: Curve 1 represents the modulus of elasticity measured in transient tests, whereby the specimens were subjected to continuous cyclic loading between 9.1 and 27.3 N/mm². Curve 2 indicated the modulus of elasticity obtained with cyclic loading between 0.2 and 18.2 N/mm². The values of curve 3 are results from so-called steady state tests (heating without external load, 2 h hold time period after reaching the test temperature, determination of the modulus of elasticity by loading and unloading the specimen three times at constant temperature). It can be seen, that the values of the modulus of elasticity obtained with different test methods yield at high temperature, e.g. 600 °C, ratios up to 1:4, with respect to equation (4) the Φ-values must be altered - according to the selected value of the modulus of elasticity in the ratio 1:4, too.

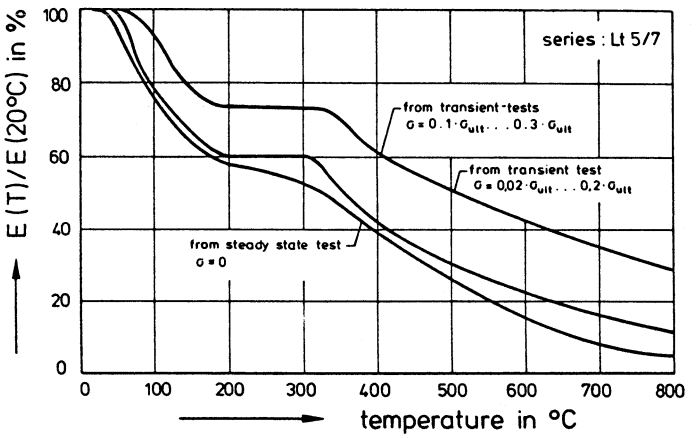


Fig. 5. Modulus of elasticity of high strength fly ash concrete determined by different test methods($\sigma_{ult}$ = 91,8 N/mm², E (20°C) = 57,7 kN/mm²

In fact, the ratio between elastic and plastic load dependent deformation reduces with increasing temperature, as it can be seen in Fig. 6, which indicates the load dependent deformations (comp. equation (1)) of a high strength concrete specimen heated under load (roughly 10 % of its ultimate load at 20 °C). From 20 °C up to 100 °C the load dependent transient deformations are nearly completely governed by the elastic modulus. In this temperature region the original modulus of elasticity is maximally reduced by 10 % ... 20 %. Above 100 °C bigger

load dependent shortenings occur; but the increase of strain due to the thermally induced reduction of the modulus of elasticity ($\sigma_0/E(\hat{\sigma}_2,T) - \sigma_0/E(20°C)$) respectively ($\sigma_0/E(\hat{\sigma}_1,T) - \sigma_0/E(20°C)$) is at 150 °C only 1/4 to 1/3 of the additionally to the initial elastic strain ($\varepsilon_{el}(20°C) = \sigma_0/E(20°C)$) occuring strain (designated $\sigma_0 \cdot \tilde{\varepsilon}/\sigma_{ult}$ in Fig. 6); at 700 °C the mentioned ratio is reduced to 1/5 to 1/25.

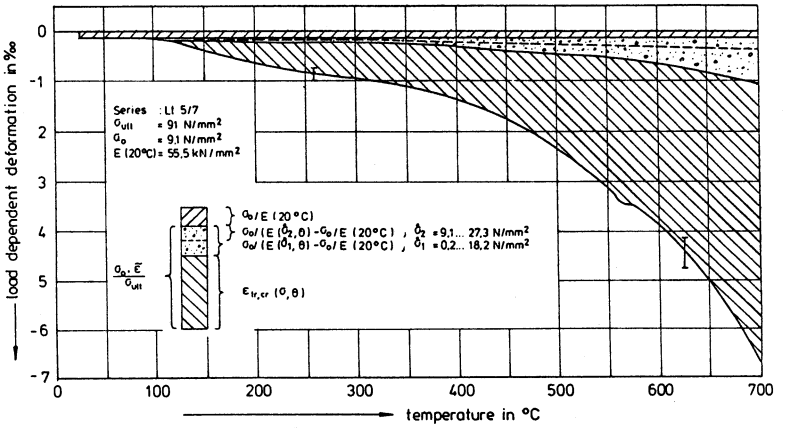


Fig. 6. Components of the load dependent deformation of high strength, fly ash concrete heated under sustained load

For the mentioned reasons and with a view to simplify the mathematical description of the transient deformation, in the following model, the strains due to thermally induced alterations of the elastic modulus ($\sigma/E(\sigma,T) - \sigma/E(20°C)$) and the other load dependent deformation components $\varepsilon_{tr}(\sigma,T)$ are combined in the term $\tilde{\varepsilon} \cdot \alpha$ respectively $\tilde{\varepsilon} \cdot \sigma/\sigma_{ult}$ (see Fig. 6). $\tilde{\varepsilon}$ represents the temperature and load dependent deformations normalized to the load level $\alpha$ (normalized transient strain). According to this definition the total deformation is composed of three components:

$$\varepsilon_{tot} = \varepsilon_{th}(T) + \varepsilon_{el}(\sigma) + \varepsilon_{tr}(\sigma,T) \tag{5}$$

respectively

$$\varepsilon_{tot} = \varepsilon_{th}(t) + \frac{\sigma}{E(20°C)} + \frac{\sigma}{\sigma_{ult}} \cdot \tilde{\varepsilon}(T) \tag{6}$$

$\varepsilon_{th}$ depends only on the temperature, $\tilde{\varepsilon}$ on the temperature and, presumably on the load level and E(20°C) as well as $\sigma_{ult}$ are constants. $\tilde{\varepsilon}$ can be determined from results of transient creep tests:

$$\tilde{\varepsilon} = (\varepsilon_{tot} - \varepsilon_{el}(20°C) - \varepsilon_{th})/\alpha \tag{7}$$

The evaluation of a series of transient tests with various mixtures has yielded, that the concrete deformations may be predicted with sufficient accuracy by equation (7). However, in some cases it seemed to be more advantageous to normalize the measured load dependent transient strains to the actual stress $\sigma$

$$\bar{\varepsilon} = (\varepsilon_{tot} - \varepsilon_{el}(20°C) - \varepsilon_{th})/\sigma \tag{8}$$

respectively in connexion with transient creep tests to the initial stress $\sigma_0$, which is maintained constant during the whole testing time with this type of tests.

$$\overline{\varepsilon} = (\varepsilon_{tot} - \varepsilon_{el}(20°C) - \varepsilon_{th})/\sigma_o \qquad (9)$$

## Evaluation and Discussion of the Test Results

The measured total strains of Rhine gravel concrete and basalt concrete are comprehensively presented in Figs. 3 and 4. Here the values at the stress level $\sigma = 0$ represent the thermal expansion. The figures with the basalt concrete show, that already at relatively low stress levels, e.g. 16.1 N/mm², the superposed transient creep strains compensate the thermal expansion of the concrete. At higher creep stresses, e.g. 26.0 N/mm² in Fig. 3, the transient creep strain already doubles the thermal expansion. Besides the values obtained with the specimens loaded with 32.2 N/mm², it can be seen, that the measured data indicate relatively low scattering.

For a better description of the various phenomena, mean values were calculated and subsequently analytically transformed to obtain exponential splines for further data processing. The used methods are comprehensively described by Wydra et al. (1985) and Weber et al. (1987).

The computed mean value curves are shown in Figs. 7 and 8. It is obvious, that - nearly independent of the stress level - all specimens expand up to 60 °C. Above 60 °C the concretes indicate transient creep of increasing magnitude. The creep rates reach their biggest values in the temperature region 90 °C ... 120 °C, where simultaneously the forced liberation of physically bound pore water occurs. After completion of the drying at about 120 °C ... 140 °C, the creep rates decrease.

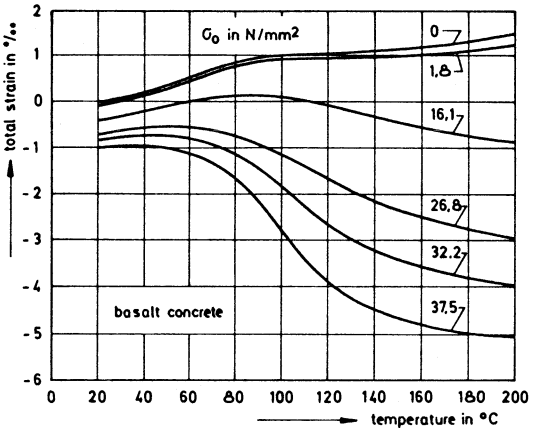


Fig. 7. Calculated mean values of the total deformations of basalt concrete

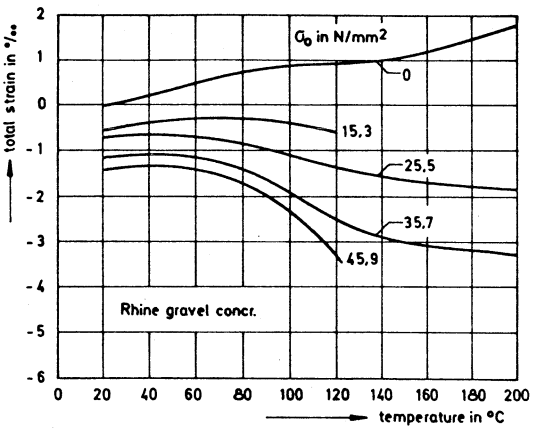


Fig. 8. Calculated mean values of total deformations of Rhine gravel concrete

For illustration, the transient creep deformations, which have been calculated according to equation (5) utilizing the thermal expansions and the measured spontaneous initial elastic strains are presented in Figs. 9 and 10. Clearly it can be seen, that the curves of the transient creep strains which were obtained with different stress levels are very similar.

The further evaluation according to the equation (9) (compare Figs. 11 and 12) shows, that with Rhine gravel concrete up to 45.9 N/mm² and with basalt concrete up to 26.8 N/mm², the magnitude of the transient creep strains depends linearly on the stress level.

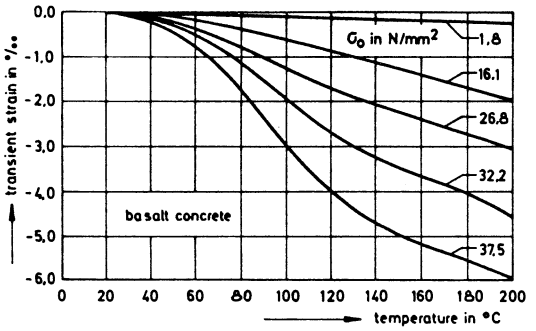


Fig. 9. Transient creep strain of basalt concrete

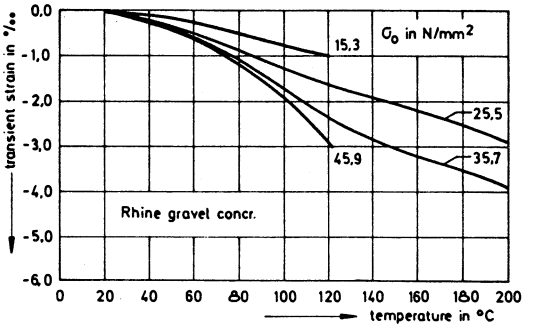


Fig. 10. Transient creep strain of Rhine gravel concrete

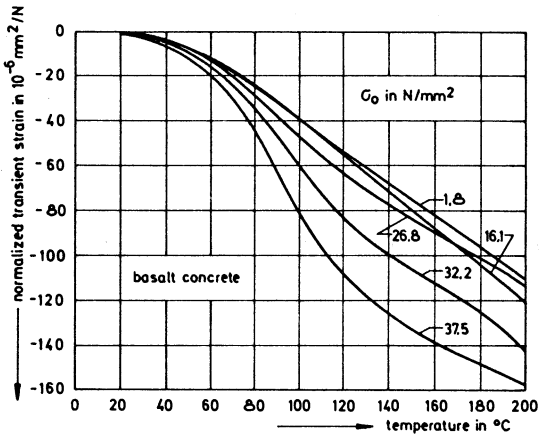


Fig. 11. Normalized transiend creep strain of basalt concrete

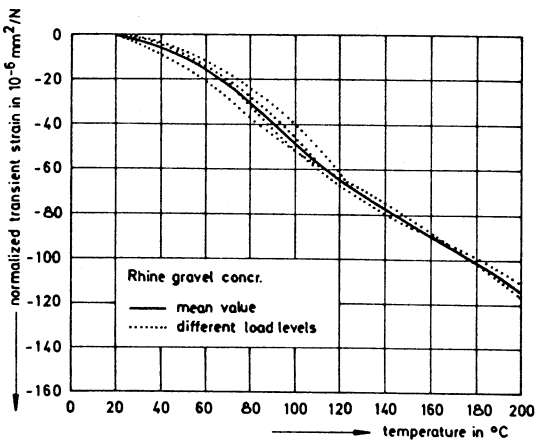


Fig. 12. Normalized transient creep strain of Rhine gravel concrete

With basalt concrete higher stress levels - in this case stress levels of 32.2 N/mm² and 37.5 N/mm², which are about 60 % respectively 70 % of the ultimate stress at 20 °C - the transient creep strains increase progressively with increasing stress. Therefore a correction function $1 + \chi$ was introduced. It is given in Fig. 13. Up to stresses of 26.8 N/mm² it runs parallelly to the stress axis. Above the stress of 26.8 N/mm² the function progressively increases with increasing stress. At about 45.6 N/mm², which represents nearly 85 % of the ultimate stress at 20 °C, the function approaches very high values and so indicates the onset of failure of the specimen under the acting creep stress.

Fig. 14 indicates the transient strain functions which were renormalized according to the following equation:

$$\bar{\varepsilon}_{tr} = \frac{\varepsilon_{tot} - \varepsilon_{el}(20°C) - \varepsilon_{th}}{\sigma_0 (1 + \chi)} \qquad (10)$$

The dotted curves show the single renormalized transient creep curves obtained with different stress levels. The full line represents the mean value curve. It can be seen, that the presented renormalization yields excellent conformity of the transient creep curves measured with different stress levels.

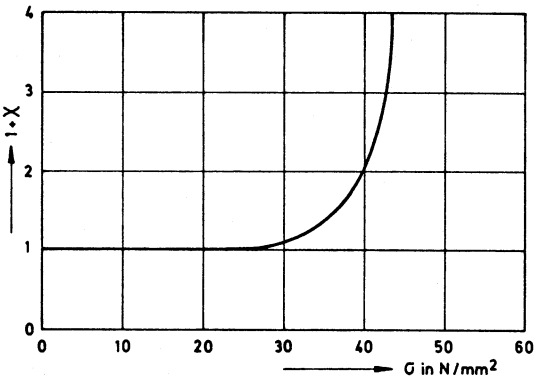


Fig. 13. Renormalization function 1 + $\chi$ for basalt concrete

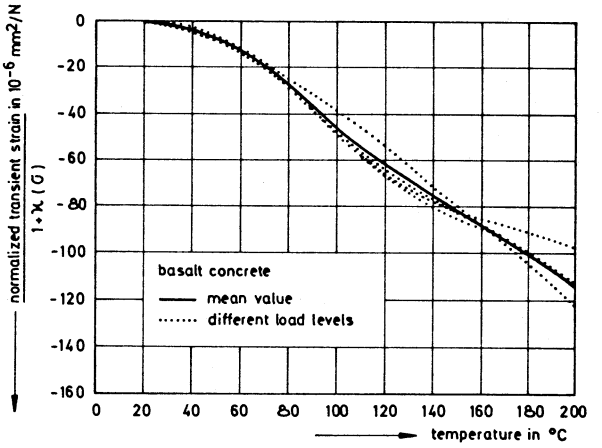


Fig. 14. Renormalized transient creep strain of basalt concrete

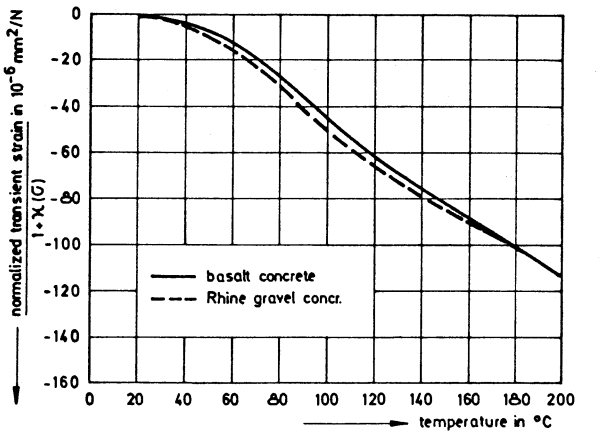


Fig. 15. Comparison of the normalized transient creep strain functions of basalt concrete and Rhine gravel concrete

A direct comparison of the normalized transient creep curves is given in Fig. 15. It is obvious, that the Rhine gravel concrete shows a little bit higher normalized transient strain than the basalt concrete. But, the two concretes differ in their normalized transient creep functions only to a very small extent, thus for rough calculations it is sufficient to use the same transient creep function in calculations for both concretes.

## CONCLUSIONS

The evaluation has revealed, that the type of the coarse mineral aggregates mainly determines the thermal expansion of the concrete, affecting, however, the transient creep deformations only to a minor extent. Thus, in cases where limited accuracy is accepted, it is sufficient to use the same transient creep function in calculations for both types of concrete. However, for more exact calculations specific effects, like higher transient creep deformation of basalt concrete at very high load level, should be taken into consideration, too.

## REFERENCES


Becker, G. (1984). R & D program for the enhancement of the safety and economics of prestressed concrete reactor vessels (PCRV). Specialists' meeting on design, criteria and experience with prestressed reactor pressure vessels for gas cooled reactors, International Atomic Energy Agency, Vienna, held in Lausanne, Switzerland (1984), IAEA-Report IWGGCR-11, Vienna 1985.

Schneider, U.; Diederichs, U.; Weber, A. (1984): Behaviour of HTR-concrete at elevated temperatures - State-of-the-Art. Specialists' meeting on Design, criteria and experience with prestressed reactor pressure vessels for gas cooled reactors. International Atomic Energy Agency, Vienna, held in Lausanne, Switzerland (1984), IAEA-Report IWGGCR-11, Vienna 1985.

Diederichs, U. (1986): HTR-Betonversuche - Dauerstandsversuche. Abschlußbericht zur Untersuchung im Auftrage der Hochtemperatur-Reaktorbau GmbH, Mannheim (FRG). Institut für Baustoffe, Massivbau und Brandschutz der Technischen Universität Braunschweig, April 1986.

Diederichs, U. (1986): HTR-Betonversuche - E-Modul-Versuche. Abschlußbericht zur Untersuchung im Auftrage der Hochtemperatur-Reaktorbau GmbH, Mannheim (FRG). Institut für Baustoffe, Massivbau und Brandschutz der Technischen Universität Braunschweig, April 1986.

Diederichs, U. (1986): HTR-Betonversuche - Hochtemperaturkriechversuche. Abschlußbericht zur Untersuchung im Auftrage der Hochtemperatur-Reaktorbau GmbH, Mannheim (FRG). Institut für Baustoffe, Massivbau und Brandschutz der Technischen Universität Braunschweig, Juni 1986.

Diederichs, U.; Ehm, C. (1986): HTR-Betonversuche - Biaxiale Druckversuche. Abschlußbericht zur Untersuchung im Auftrage der Hochtemperatur-Reaktorbau GmbH., Mannheim (FRG), Institut für Baustoffe, Massivbau und Brandschutz der Technischen Universität Braunschweig, Juni 1986.

Weber, A.; Wydra, W.; Diederichs, U. (1985): A contribution to the analytical description of concrete deformation under transient temperatures. Proceedings of the 8th International Conference on "Structural Mechanics in Reactor Technology", Lausanne (Switzerland), 17 - 21 August 1987, Volume H, pp. 121-126, 1987.

Anderberg, Y.; Thelandersson, S. (1976): Stress and deformation characteristics of concrete at high temperatures. 2. Experimental Investigation and material behaviour model. Lund Inst. of Technology, Division of Structural Mechanics and Concrete Construction, Bulletin 54, Lund 1976.

Khoury, G.A.; Grainger, B.N.; Sullivan, P.J.E. (1985): Strain of Concrete during the first heating to 600 °C under load. Magazine of Concrete Research, Vol. 37, No. 133, pp. 195-215, December 1986.

Jumppanen, U.M.; Diederichs, U.; Hinrichsmeyer, K. (1986): Material Properties of F-Concrete at High Temperatures. VTT Research Reports 452, Technical Research Centre of Finland, Espoo (Finland), 1986.

Schneider, U. (1988): Concrete at High Temperatures - A General Review, Fire Safety Journal, 13 (1988), pp. 55-58.
Diederichs, U.; Becker, G.; Weber, A. (1987): High-temperature creep behaviour of HTR-concrete. Transactions of the 9th International Conference on "Structural Mechanics in Reactor Technology", Lausanne (Switzerland), 17 - 21 August, Volume H, pp. 115-120, 1987.
Diederichs, U.; Ehm, C.; Weber, A.; Becker, G. (1987): Deformation behaviour of HTR-concrete under biaxial stresses and elevated temperatures. Transactions of the 9th International Conference on "Structural Mechanics in Reactor Technology", Lausanne (Switzerland), 17 - 21 August, Volume H, pp. 109-114, 1987.
Diederichs, U.; Jumppanen, U.M.; Penttala, V. (1989): Behaviour of high strength concrete at high temperatures. Helsinki University of Technology, Department of Structural Engineering, Report 92, Espoo (Finland), 1989.
Wydra, W.; Diederichs, U.; Schneider, U. (1985): Deformation behaviour and creep effects during a heating-cooling-cycle. Proceedings of the 8th International Conference on "Structural Mechanics in Reactor Technology", Brussels (Belg.), 19 - 23 August 1985, Volume 4, paper H 5/6, 1985.